INFLUENCE OF MATERIAL ATTACHMENT FOR EM ABSORPTION

Mohammad Rashed Iqbal Faruque[1], Mohammad Tariqul Islam [2], Norbahiah Misran[1, 2]

[1]Dept. of Electrical, Electronic and Systems Engineering, Faculty of Engineering and Built Environment, Universiti Kebangsaan Malaysia, Bangi, Selangor, Malaysia.
[2]Institute of Space Science (ANGKASA), Universiti Kebangsaan Malaysia, Bangi, Selangor, Malaysia.

Key words: antenna, human head model, lossy-Drude model, materials, SAR.

Abstract: In this paper, reducing electromagnetic absorption (EM) with materials attachment is investigated. The finite-difference time-domain method with lossy-Drude model is adopted in this study. The methodology of SAR reduction is addressed and the effects of attaching location, distance, and size of ferrite sheet material on the SAR reduction are investigated. Materials have achieved a 47.68% reduction of the initial SAR value for the case of 1 gm SAR. These results suggest a guideline to choose various types of materials with the maximum SAR reducing effect for a phone model.

Vpliv feritnega dodatka na EM absorpcijo

Kjučne besede: antena, človeški model glave, model lossy-Drude, materiali, SAR

Izvleček: v članku raziskujemo vpliv dodatnih pritrjenih materialov na EM absorpcijo. Pri simulaciji smo uporabili dva modela. S pomočjo metodologije SAR zasledujemo vpliv položaja, razdalje in velikosti ploskih feritnih materialov na zmanjševanje SAR. Dodani materiali zmanjšajo za 47.68 % začetno SAR vrednost v primeru 1g SAR. S pomočjo teh rezultatov pridemo do smernic pri izbiri materialov za doseganje največjega SAR zmanjšanja za model telefona.

1. Introduction

Sources of radio frequency/microwave (RF/MW) radiation, particularly cellular phones are ever present. RF/MW sources are part of daily life, but they also reason for concern regarding the possible biological effects of microwaves. It is important that the biological effects of RF/MW fields are minimal, at least at the level of their clinical significance, so that health risk can be assessed. Because the potential shock of RF/MW fields on human health has not yet been well characterized, the basic knowledge from laboratory studies based on cellular and animal test systems are invaluable. The interaction of handset antennas with the human body is a great consideration in cellular communications. The user's body, especially the head and hand, influence the antenna voltage standing wave ratio (VSWR), gain, and radiation patterns. Furthermore, thermal effects, when tissues are exposed to unlimited electromagnetic energy, can be a serious health hazard. Therefore standards organizations have set exposure limits in terms of SAR /1, 2/. SAR is a measure of the rate at which radio frequency (RF) energy is absorbed by the body when exposed to a radio-frequency electro-magnetic field. SAR is used to measure exposure to fields between 100 kHz and 10 GHz /3-5/. It is commonly used to measure power absorbed from mobile phones and during MRI scans. The value will depend on the geometry of the part of the body that is exposed to the RF energy, and on the exact location and geometry of the RF source.

Cellular phone protection and the enforcement of pertinent exposure standards are issues in the current media, and regulatory agencies are motivated to assure that compliance testing is acceptable. IEEE Standard 1528 /1/ and IEC 62209-1 specify protocols and process for the measurement of the peak spatial-average SAR induced inside a simplified model of the head of users of hand held radio transceivers (cellular phones). For example, the SAR limit specified in IEEE C95.1: 1999 is 1.6 W/kg in a SAR 1 gm averaging mass while that specified in IEEE C95.1: 2005 has been updated to 2 W/kg in a 10 gm averaging mass /2/. This new SAR limit specified in IEEE C95.1: 2005 is comparable to the limit specified in the International Commission on Non-Ionizing Radiation Protection (ICNIRP) guidelines.

The exposure limits are defined commonly in terms of the spatial peak SAR averaged either over any one gram or ten grams of tissue. Since 1997, the U.S. Federal Communication Commission (FCC) requires the routine SAR evaluation of a phone model prior to device authorization or use. So there is a need to reduce the spatial peak SAR in the design stage of a phone model because the possibility of a spatial peak SAR exceeding the recommended exposure limit cannot be completely ruled out /2/, /3-5/. The interaction of the cellular handset with the human head has been investigated by many published papers considering; first, the effect of the human head on the handset antenna performance including the feed-point impedance, gain, and efficiency /6-10/, and second, the impact of the antenna EM radiation on the user's head due to the absorbed power, which is measured by predicting the induced SAR in the head tissue /9-13/.

The most used method to solve the electromagnetic problem in this area is the finite-difference time-domain (FDTD) technique /12-13/. Although, in principle, the solution for general geometries does not require any additional effort with respect to the standard method, the technique requires the definition of a discretized space by assigning to each cell its own electromagnetic properties, which is not an easy process /14-16/. Specifically, the problems to be solved in SAR reduction need a correct representation of the cellular phone, anatomical representation of the head, alignment of the phone and the head, and suitable design of materials or metamaterials.

Human exposure to electromagnetic (EM) radiation, as well as the pertinent health effects, constitutes a matter of raised public concern, and this issue has undergoing continuous scientific investigation. Various studies on this subject exist /14–17/, most of which mainly investigate into the consequences of mobile-phone usage. Yet, devices and communication terminals operating in other frequency bands have also gained substantial interest in the last 15 years. In /8/, a ferrite sheet was adopted as protection between the antenna and the human head. A reduction of over 13% for the spatial peak SAR over 1 gm averaging was achieved. A study on the effects of attaching a ferrite sheet for SAR reduction was presented in /15/, and it was concluded that the position of shielding plays an important role in the reduction effectiveness.

In /17/, for the SAR in the human head, an effective approach is the use of a planar antenna integrated onto the back side (away from the head) of a phone model, but it brings additional design difficulties especially in achieving the required frequency bandwidth and radiation efficiency. Another approach is the use of a directional or reflecting antenna /15-16/. Such an antenna structure sacrifices the availability of signals received from all directions to the phone model. The mechanism of SAR reduction by ferrite sheet attachment was due to the suppression of surface currents on the front side of phone model /18/. However, the relationship between the maximum SAR reducing effect and the parameters such as attaching location, size and material properties of ferrite sheet remains unknown.

In /11/,/18/ a perfect electric conductor (PEC) reflector was placed between a human head and the driver of a folded loop antenna. The result showed that the radiation efficiency can be enhanced and the peak SAR value can be reduced. In /14/, a study on the effects of attaching conductive materials to cellular phone for SAR reduction has been presented. It is shown that the position of the shielding material is an important factor for SAR reduction effectiveness. There is a necessity to make an effort for reducing the spatial peak SAR in the design stage of ferrite sheet because the possibility of a spatial peak SAR exceeding the recommended exposure limit cannot be completely ruled out.

This paper is structured as follows. Section II describes the numerical analysis of the handset together with the SAM phantom head. The FDTD method is used with positive meshing techniques for quick and correct analysis. The modeling and analyzing technique will be described in Section III. Simulation and comparing results of materials will be summarized in Section IV and Section V concludes the paper.

2. Simulation model and numerical techniques

A. Model Description

The simulation model which includes the handset with PIFA type of antenna and the SAM phantom head provided by CST Microwave Studio® (CST MWS) is shown in Fig. 1. A complete handset model composed of the circuit board, LCD display, keypad, battery, and housing was used for simulation. The relative permittivity and conductivity of individual components were set to comply with industrial standards. In addition, definitions in /3-4/, /17/ were adopted for material parameters involved in the SAM phantom head. In order to accurately characterize the performance over a broad frequency range, dispersive models for all the dielectrics were adopted during the simulation /3/. Fig. 2 shows the dispersive permittivity of the liquid in the SAM phantom head for simulation. In Fig. 2, Eps' and Eps'' represents dielectric dispersion fit Debye 1st order and 2nd order respectively. The electrical properties of materials used for simulation are listed in Table 1. A PIFA type antenna constructed in a helical sense operating at 900 MHz for GSM application was used in the simulation model. In order to obtain a high-quality geometry approximation for such a helical structure, a predictable meshing scheme used in the FDTD method usually requires large number of hexahedrons which in turn makes it extremely challenging to get convergent results within reasonable simulation time.

Fig. 1: Complete model used for simulation including handset and SAM phantom head.

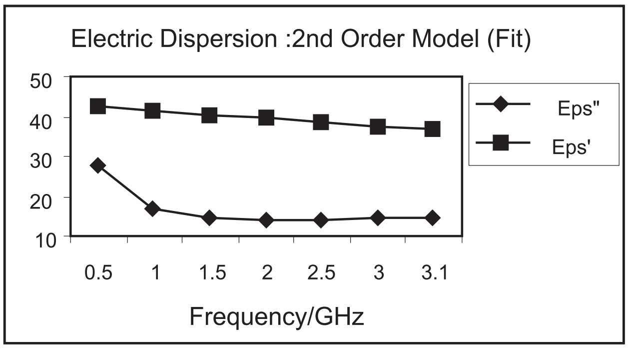

Fig. 2: Dispersive permittivity of the liquid in the SAM phantom head used for simulation.

Table 1: Electrical properties of materials used for simulation

Phone Materials	ε_r	σ (S/m)
Circuit Board	4.4	0.05
Housing Plastic	2.5	0.005
LCD Display	3.0	0.02
Rubber	2.5	0.005
SAM Phantom Head		
Shell	3.7	0.0016
Liquid @ 900MHz	40	1.42

B. Numerical Technique

CST MWS, based on the finite integral time-domain technique (FITD), was used as the main simulation instrument. A non-uniform meshing scheme was adopted so that the major computation endeavor was dedicated to regions along the inhomogeneous boundaries for fast and perfect analysis. Fig. 3 shows the mesh for two cut planes of the complete model indicating the area with denser meshing along the inhomogeneous boundaries. The minimum and maximum mesh sizes were 0.3 mm and 1.0 mm, respectively. A total of 2,097,152 mesh cells were generated for the complete model, and the simulation time was 1163 seconds (including mesh generation) for each run on an Intel Core™ 2 Duo E 8400 3.0 GHz CPU with 4 GB RAM system.

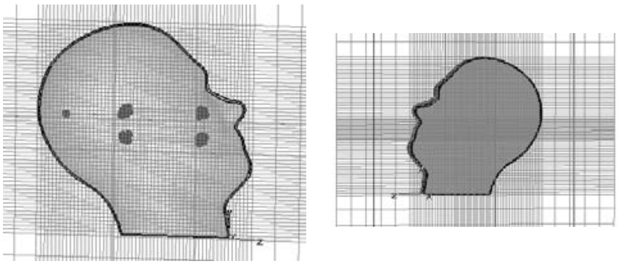

Fig. 3: Mesh view for two cut planes of the complete model showing the non-uniform meshing scheme adopted for simulation.

The analysis workflow started from the design of the antenna with complete handset model in free space. The antenna was designed such that the *S*11 response was less than -10 dB over the frequency band of interest. The SAM phantom head was then included for SAR calculation using the standard definition as /5/

$$SAR = \frac{\sigma}{2\rho} E^2$$

where *E* is the induced electric field (V/m), ρ is the density of the tissue (kg/m^3), and σ is the conductivity of the tissue (S/m). The resultant SAR values averaged over 1 gm and 10 gm of tissue in the head were denoted as SAR 1 gm and SAR 10 gm, respectively. These values were used as a benchmark to appraise the effectiveness in peak SAR reduction.

3. Sar reduction with lossy drude model

A. Lossy-Drude Model

The SA reduction effectiveness and antenna performance with different positions, sizes, and material properties of materials and metamaterials will be analyzed. The head models used in this study were obtained from a MRI-based head model through the whole brain Atlas website. Six types of tissues, i.e., bone, brain, muscle, eye ball, fat, and skin were involved in this model /17-19/. Table II shows their dielectric properties. Fig. 4 shows a horizontal cross-section through the eyes of this head model. The electrical properties of tissues were taken from /13/. Numerical simulation of SAR value was performed by the FDTD method. The parameters for FDTD computation were as follows. In our Lossy-Drude simulation model, the domain was 128 x 128 x 128 cells in the FDTD method. The cell sizes were set as $\Delta x = \Delta y = \Delta z$ = 1.0 mm. The computational domain was terminated with 8 cells perfectly matched layer (PML). A PIFA antenna was modeled for this paper by the thin-wire approximation. Simulations of materials and metamaterials are performed by the FDTD method with the lossy-Drude model /19/. The method is utilized to understand the wave propagation characteristics of materials and metamaterial.

Table 2: Dielectric tissue properties at 900 MHz

Material	Density, ρ (Kg-m^{-3})	Conductivity, σ (S-m^{-1})	Relative permittivity ε_r
Fat, bone	1130	0.12	4.83
Muscle, skin	1020	1.5	50.5
Brain	1050	1.11	41.7
Eye ball	1000	2.03	68.6

B. Analysis Method

Fig. 5 shows a portable telephone model at 900 MHz for the present study. It was considered to be a quarter wavelength PIFA antenna mounted on a rectangular conducting box. The conducting box was 10 cm tall, 4 cm wide, and 3

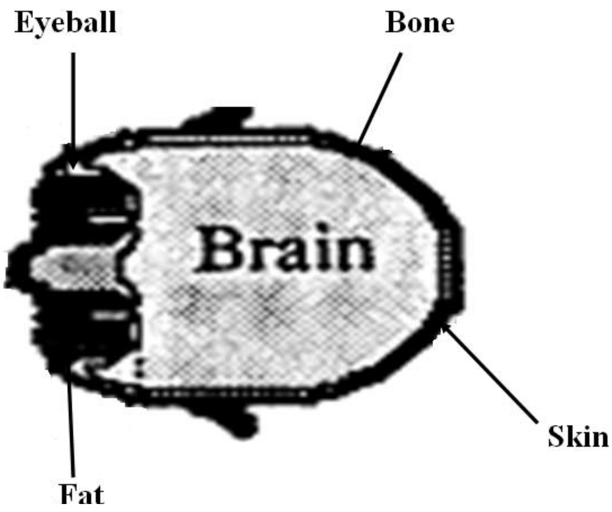

Fig. 4: Human head model for FDTD computation.

cm thick. The PIFA antenna was located at the top surface of the conducting box. A ferrite sheet with a height of 90 mm, a width of 40 mm, and a thickness of 3.5 mm was attached to the conducting box as shown in Fig. 5.

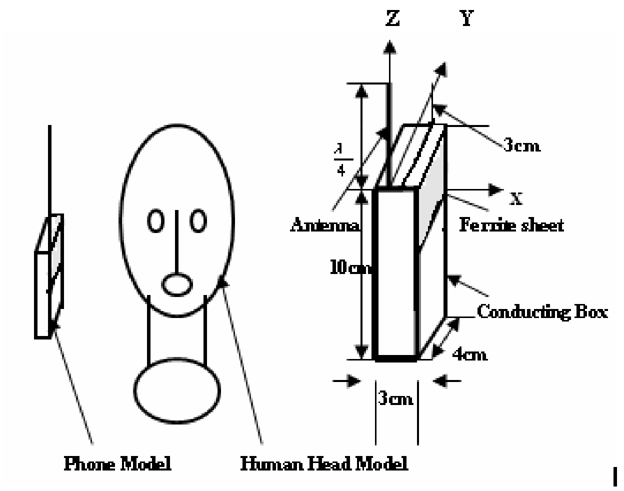

Fig. 5: odels of the head and portable telephone with an attached ferrite sheet.

The SAM head model was considered for this research where it consists about 2,097,152 cubical cells with a resolution of 1 mm. The FDTD method was employed in the numerical analysis. Its discretized formulations were derived from the following Maxwell's time-domain equations:

$$\frac{\delta H}{\delta t} = -\frac{1}{\mu_0 \mu_r'}(\nabla \times E) - \frac{\sigma^*}{\mu_0 \mu_r'} H. \quad (1)$$

$$\frac{\delta E}{\delta t} = -\frac{1}{\varepsilon_0 \varepsilon_r'}(\nabla \times H) - \frac{\sigma^*}{\varepsilon_0 \varepsilon_r'} E. \quad (2)$$

where $\sigma^* = \omega \mu_0 \mu_r''$ and $\sigma = \omega \varepsilon_0 \varepsilon_r''$. A space domain enclosing the human head and the phone model is also shown in Fig. 5. The time step was set to $\frac{\delta}{\sqrt{3c}}$, where *c* is the speed of light, to guarantee the numerical stability. The time-stepping was performed for about eight sinusoidal cycles in order to reach a steady state. To absorb outgoing scattered waves, the second order Mur absorbing boundaries acting on electric fields were used. An antenna excitation was introduced by specifying a sinusoidal voltage across the one-cell gap between the helix and the top surface of the conducting box.

The antenna output power is defined as

$$P_{out} = P_{abs} + P_{ferr} + P_{rad}$$

$$\frac{1}{2}\int_{Vh} \sigma |E|^2 \, \mathrm{dv} + \frac{1}{2}\int_{Vf} (\sigma |E|^2 + \sigma^* |H|^2) \, \mathrm{dv} + \frac{1}{2}\mathrm{Re}\left(\int_s E \times H^* . \vec{n} . \mathrm{ds}\right) \quad (3)$$

where P_{abs} is the power absorbed in the head with a volume of V_h, P_{ferr} is the power dissipated in the ferrite sheet with a volume of V_f, and $P_{rad.}$ is the power radiated to the far-field, which can be calculated by integrating the normal component of the Pointing vector *E* x *H** over a surface S completely surrounding the head/phone model configuration.

4. Impact on sar of ferrite sheet attachment

In this section, a ferrite sheet is placed between the antenna and a human head thus reducing the SAR value. In order to study SAR reduction of an antenna operated at the GSM 900 band, different positions, sizes, and ferrite sheet materials for SAR reduction effectiveness are also analyzed by using the FDTD method in conjunction with a detailed human head model.

Fig. 6 shows the simulation model which includes the handset with monopole type PIFA antenna and the SAM phantom head provided by CST MWS.

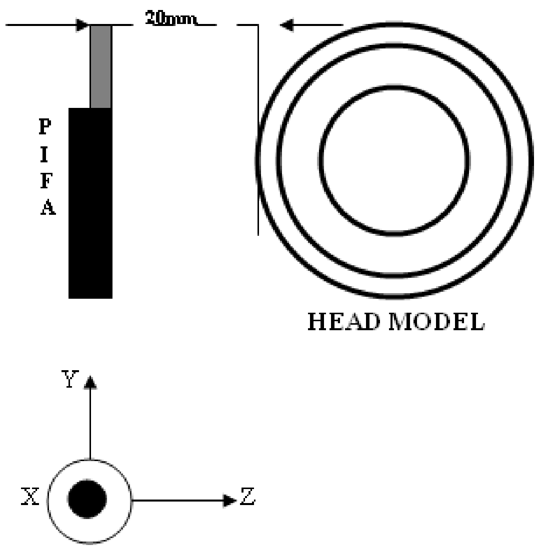

Fig. 6: The head and antenna model for SAR calculation.

The dispersive models for all the dielectrics were adopted during the simulation in order to accurately characterize the ferrite sheet. The antenna was arranged in parallel to the head axis, the distance is varied from 5 mm to 20 mm, and finally 20 mm was chosen for comparison with the ferrite sheet. Besides that, the output power of the mobile phone model needs to be set before SAR is simulated. In this paper, the output power of the cellular phone is 500 mW at the operating frequency of 900 MHz In the real case, the output power of the mobile phone will not exceed 250 mW for normal use, while the maximum output power can reach to 1 W or 2 W when the base station is far away from the mobile station (cellular phone). Without ferrite sheet, the SAR simulation is compared with the results in /6, 17 / for validation, as shown in Table III also with ferrite sheet, the SAR simulation is compared with the result of /8/ for validation, as shown in Table IV. The calculated peak SAR 1 gm value is 2.002 W/kg, and SAR 10 gm value is 1.293 W/kg when the phone model is placed 20 mm away from the human head model without a ferrite sheet. This SAR value is better compared with the result reported in /13/, which is 2.43 W/kg for SAR 1 gm. The ferrite sheet material is utilized in between the phone and head models, and it is found that the simulated value of SAR 1 gm and SAR 10 gm are 1.043 W/kg and 0.676 W/kg respectively. The reduction about of 47.68% was observed in this study when a ferrite sheet is attached between the phone and human head models for SAR 1 gm. This SAR reduction is better than the result reported in /8/, which is 13% for SAR 1 gm. This is achieved using different radiating powers and impedance factors and it is because the electromagnetic source is being moved away from the head. Figs. 7-11 show the SAR value compared with the distance between phone and head models, width of ferrite sheet between 20-40 mm, thickness of ferrite sheet between 2-3.5 mm, and height between 40-90 mm respectively.

Table 3: Comparisons of peak sar at 900 mhz without ferrite sheet

Tissue	SAR value (W/kg)
SAR value for [6]	2.17
SAR value for [17]	2.28
SAR value this work for 1 gm	2.002

Table 4: Comparisons of peak sar at 900 mhz with ferrite sheet

Tissue	SAR value (W/kg)
SAR value for [8]	1.392
SAR value this work for 1 gm	1.043

The reduction efficiency of the SAR depends on its width and height. In order to definitely confirm this, 1 gm and 10 gm average SAR versus distance, width, thickness, and height are plotted in the Figs. 7-11. In Fig. 7, it is shown that if the distance between phone and human head models is varied then the SAR value decreases. This is because the dielectric constant, conductivity, density and magnetic tangent losses are also varied. In Fig. 8, it can be observed that the SAR value reduces with the increase of the width of the ferrite sheet. As shown in Fig. 9, the SAR value decreases until a thickness of 3 mm, and then a different tendency i.e., it started to increase after 3 mm. The height is varied up to 90 mm in Fig. 10. From this figure it can be shown that if the height of the ferrite sheet increases, then the SAR value also decreases up to a height of 80 mm, and it started to increase after 80 mm. Fig. 11 shows the SAR value with ferrite sheet attachment for 1 gm and 10 gm average SAR. It can be observed that with ferrite sheet attachment the SAR value has been decreased for the case of 1 gm and 10 gm average SAR. The results implies that only suppressing the maximum current on the front side of the conducting box contributes significantly to the reduction of spatial peak SAR. This is because the decreased quantity of the power absorbed in the head is considerably larger than that dissipated in the ferrite sheet and it is because the electromagnetic source is being moved away from the head.

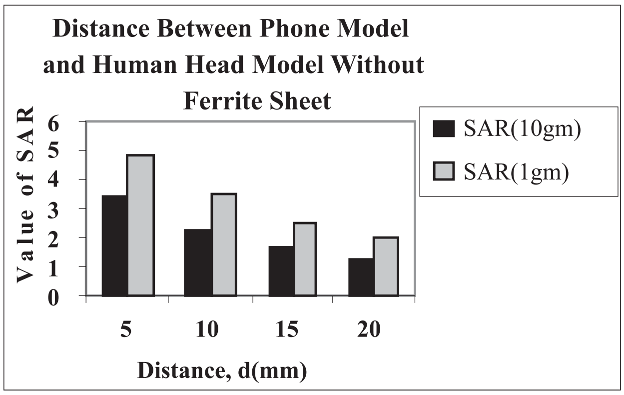

Fig. 7: SAR value compared with the distance between phone model and human head model without ferrite sheet.

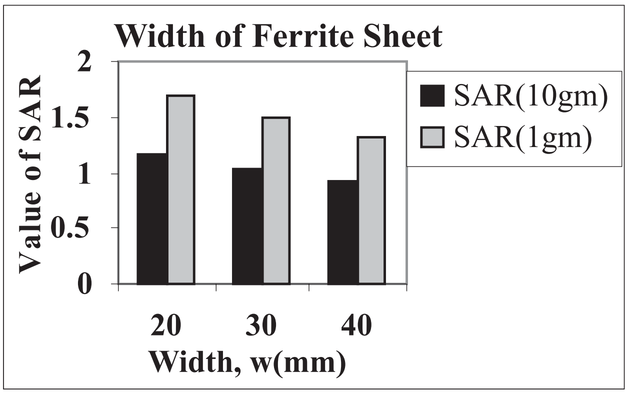

Fig. 8: SAR value compared with the width of the ferrite sheet.

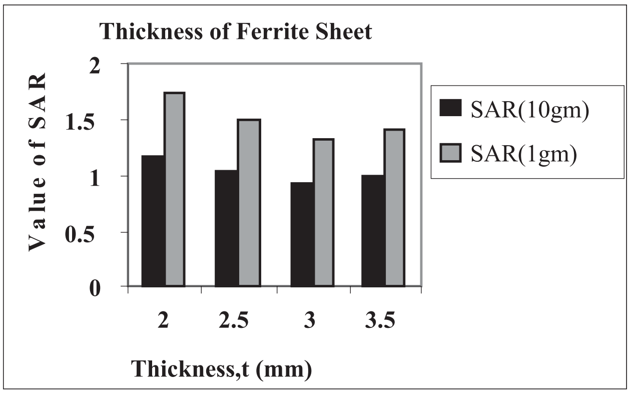

Fig. 9: SAR value compared with the thickness of the ferrite sheet.

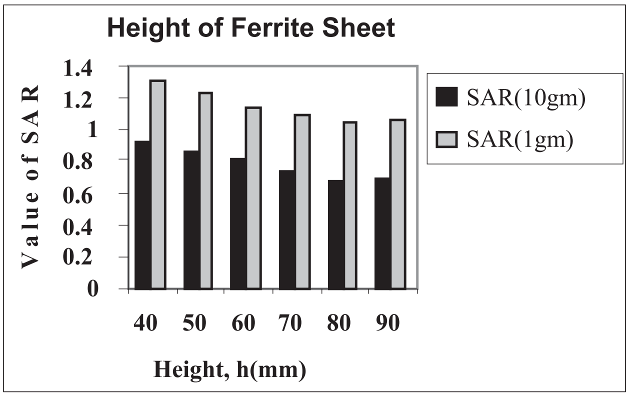

Fig. 10: SAR value compared with the height of the ferrite sheet.

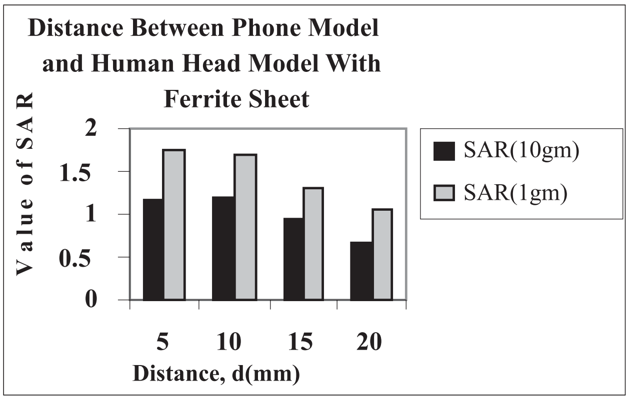

Fig. 11: SAR value compared with the distance between phone model and human head model with ferrite sheet.

5. Conclusion

The EM interaction between an antenna and the human head with ferrite sheet material has been discussed in this paper. Utilizing material in the phone model a SAR value is achieved of about 0.676 W/kg for SAR 10 gm and 1.043 W/kg for SAR 1 gm. Based on the 3-D FDTD method with lossy-Drude model, it is found that for the both cases peak SAR 1 gm and SAR 10 gm of the head can be reduced by placing materials between the antenna and the human head. Numerical results can provide useful information in designing communication equipment for safety compliance.

Acknowledgement

The authors would like to thank Institute of Space Science (ANGKASA), Universiti Kebangsaan Malaysia (UKM) and the MOSTI Secretariat, Ministry of Science, Technology and Innovation of Malaysia, e- Science fund: 01-01-02-SF0566, for sponsoring this work.

References

/1/ IEEE C95.1-2005. "IEEE Standards for safety levels with respect to Human Exposure to Radio Frequency Electromagnetic fields,3KHz to 300GHz," *Institute of Electrical and Electronics Engineers*, Inc. New York, NY 2005.

/2/ International Non-Ionizing Radiation Committee of the International Radiation Protection Association, "Guidelines on Limits on exposure to radio frequency electromagnetic fields in the frequency range from 100KHz to 300GHz," *Health Physics,* vol.54 no. 1, pp. 115-123, 1988.

/3/ A. Hirata, T. Adachi, and T. Shiozawa, "Folded loop antenna with a reflector for mobile handsets at 2.0 GHz," *Microwave Opt. Technol, Lett.*, vol.40, no.4, pp. 272-275, Feb. 2004.

/4/ K .H. Chan, K .M .Chow, L .C .Fung, and S. W. Leung, "Effects of using conductive materials for SAR reduction in mobile phones," *Microwave Opt. Technol, Lett.*, vol.44, no. 2, pp. 140-144, Jan. 2005.

/5/ L.C Fung, S .W. Leung, and K. H. Chan, "An investigation of the SAR reduction methods in mobile phone application," *IEEE International Symposium on EMC.*, vol.2, pp. 656-660, Aug. 2002.

/6/ J. Wang and O. Fujiwara, "FDTD computation of temperature rise in the human head for portable telephones," *IEEE Trans. Microwave Theory Tech*., vol. 47, no. 8, pp. 1528-1534, Aug.1999.

/7/ S. Curto, P. McEvoy, X. L. Bao, and M. J. Ammann, "Compact patch antenna for electromagnetic interaction with human tissue at 434 MHz," *IEEE Trans. on Antennas and Propagation*, vol. 57, no. 9, Sep. 2009.

/8/ J. Wang and O. Fujiwara, "Reduction of electromagnetic absorption in the human head for portable telephones by a ferrite sheet attachment," *IEICE Trans. Commun.*, vol. E80b, no. 12, pp. 1810-1815, Dec. 1997.

/9/ K Kiminami, T Iyama, T Onishi, and S Uebayashi, "Novel specific absorption rate (SAR) estimation method based on 2-D scanned electric fields," *IEEE Trans. on Electromagnetic Compatibility.,* vol. 50, no. 4, Nov. 2008.

/10/ R. G. Vaughan, and N. L. Scott, "Evaluation of Antenna Configurations for Reduced Power Absorption in the Head," *IEEE Trans. On Vehicular Technology,* vol. 48, no. 5, Sep. 1999

/11/ C. H. Li, N. Chavannes, and N. Kuster, "Effects of hand phantom on mobile phone antenna performance," *IEEE Trans. On Antennas and Propagation*, vol. 57, no. 9, Sep. 2009.

/12/ O. Kiverkas, J. Ollikainen, T. Lehtiniemi, and P. Vainikainen, "Bandwidth, SAR, and efficiency of internal mobile phone antennas," *IEEE Trans. on Electromagnetic Compatibility.*, vol. 46, no. 1, Feb. 2004.

/13/ J. N. Hawang and Fu-chiarng chen. "Reduction of the peak SAR in the Human Head with Metamaterials" *IEEE Trans. on antenna and propagation* vol. 54 (12) 3763-3770, Dec. 2006.

/14/ L. C. Fung, S. W. Leung, and K. H. Chan, "Experimental study of SAR reduction on commercial products and shielding materials in mobile phone applications," *Microwave and Optical Technology Letters*, vol. 36, no. 6, pp. 419-422, March. 2003.

/15/ J. B. Pendry, A. J. Holen, D. J. Robbins, and W. J. Stewart, "Magnetism from conductors and enhanced nonlinear phenomena," *IEEE Trans. Microwave Theory Tech.*, vol. 47, no. 11, pp. 2075–2084, Nov. 1999.

/16/ G.F. Pedersen and J.B. Andersen, "Integrated antennas for hand-held telephones with low absorption", *Proc. 44th IEEE Veh. Tech. Conf.,* Stockholm, Sweden, June. 1994, pp. 1537-1541.

/17/ C .M .Kuo. and C. W. Kuo, "SAR distribution and temperature increase in the human head for mobile communication," *in IEEE-APS* Int. Symp. Dig., Columbus, OH, 2003, pp. 1025-1028.

/18/ R. Y. S. Tay, Q. Balzano and N. Kuster, "Dipole configuration with strongly improved radiation efficiency for hand-held transceivers", *IEEE Trans. Antennas Propagat.*, vo1. 46, no. 6, pp. 798-806, June. 1998.

/19/ B. B. Beard, W. Kainz, T. Onishi, T. Iyama, S. Watanabe, O. Fujiwara, J. Wang, G. Bit-Babik, A. Faraone, J. Wiart, A. Christ, N.Kuster, A. Lee, H. Kroeze, M. Siegbahn, J. Keshvari, H. Abrishamkar, W. Simon, D. Manteuffel, and N. Nikoloski, " Comparisons of computed mobile phone induced SAR in the SAM phantom to that anatomically corrects model of the human head," *IEEE Transaction on Electromagnetic Compatibility*, vol. 48, no.2, pp 397-407, 2006.

Mohammad Rashed Iqbal Faruque[1],
Mohammad Tariqul Islam[2],
Norbahiah Misran[1, 2]

[1]Dept. of Electrical, Electronic and Systems Engineering, Faculty of Engineering and Built Environment, Universiti Kebangsaan Malaysia, 43600 UKM, Bangi, Selangor, Malaysia.
[2]Institute of Space Science (ANGKASA), Universiti Kebangsaan Malaysia, 43600 UKM, Bangi, Selangor, Malaysia.

rashedgen@yahoo.com,
titareq@yahoo.com,
bahiah@vlsi.eng.ukm.my

Prispelo: 05.02.2010 *Sprejeto: 03.03.2011*